Evaluation of Trends in Optimal Design of Pulse Transformers for Long Pulse High Power Applications

Max Collins

Industrial Electrical Engineering and Automation
Lund University
Lund, Sweden

Carlos. A Martins(*)

Power Converters Section, Accelerator Division
European Spallation Source ERIC
Lund, Sweden

(*) and Industrial Electrical Engineering and Automation, Lund University

Abstract— **Solid state klystron modulators are typically based on oil-immersed pulse transformers due to their high performance, robustness, simplicity and straightforward design. However, the size of such transformers are highly impacted by pulse power, output voltage, pulse length, and required rise time; key parameters which are difficult to combine in long pulse high power linac applications. In this paper, pulse transformer design models for two winding configurations (single layer winding and pancake winding), including calculation of parasitic elements, are developed and validated in a 3D finite element analysis environment. These models are then employed in a global optimal design procedure used to study the evolution of pulse transformer volume as pulse length is increased from 500 µs to 4 ms while constraining maximum pulse rise time and overshoot. The impact of required pulse power, pulse rise time, and system size is also studied. The single layer winding based on standard enameled round wire is first investigated under size constraints representing a limit imposed by manufacturability and maintainability, validating the optimization procedure and demonstrating that, for this winding technique, sub-optimal rise time and therefore transformer size is attained for long pulse high power applications. Consequently, the pancake winding configuration is evaluated under the same conditions, demonstrating that, although more complex and costly, its flexibility allows a more compact design. Finally, a pulse transformer rated for pulse amplitude 115 kV, output current 25 A, pulse length 2.8 ms, and 0-99% rise time <300 µs is designed, demonstrating the design procedure and showcasing limitations experienced in design. Its performance is assessed in circuit simulation whereas the validity of the derived parameters is demonstrated through finite element analysis.**

Keywords—Accelerator power supplies, high voltage techniques, pulse power systems, pulse generation

I. INTRODUCTION

Pulsed klystron modulators used in linear accelerators are required to produce pulsed power of a given pulse length and pulse repetition rate, featuring short rise time, low pulse overshoot, and very low flat top ripple and droop. Such modulators are based on solid state technology, integrating a capacitor charger followed by a pulse generation and voltage amplification stage [1]. In most applications, a pulse transformer based approach is favored due to their high performance, robustness, simplicity, and straightforward design. Here, the output stage is implemented by a solid state switch, a monolithic pulse transformer, as well as a number of auxiliary systems for pulse droop compensation and transformer demagnetization, Fig. 1.

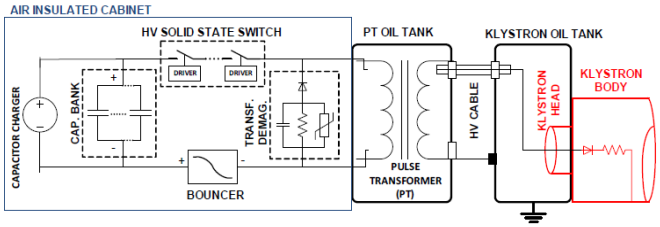

Fig. 1. Pulse transformer based topology

Key pulse parameters are highly application-dependent, with e.g. required pulse length varying from the sub-microsecond range up to several milliseconds [2][3][4][5], derived from the needs of the end physics users. Hence, some type of optimization procedure is often a necessity to ensure good design [6][7][8]. In addition, the quality of the output pulse is strongly determined by the pulse transformer, demanding accurate models for estimation of stray capacitance and leakage inductance [9][10], as well as a method for choosing appropriate construction.

Some applications, e.g. spallation, require a combination of high pulse power and long pulse length, [11][12], with the desire for compact component design (i.e. increased power density). These requirements imply challenging pulse transformer design as the monolithic transformer is required to sustain the entire voltage time area of the pulse. In addition, pulse rise time and pulse overshoot are uniquely determined by modulator load impedance and transformer parasitic elements, constraining the geometry of the transformer windings. Hence, as pulse length and therefore resulting voltage time area increase, the restrictions on transformer winding configuration, and in particular number of turns, imply steep increase in size, limited by manufacturability and maintainability.

II. Pulse Transformer Optimization

In this section, an optimal design procedure is developed for pulse transformers based on the single layer winding and pancake winding techniques. The procedure is based on the MATLAB® Optimization Toolbox™, utilizing the fmincon solver. In this problem formulation, the solver is set to minimize the volume function of the pulse transformer while constraining pulse rise time, pulse overshoot, and transformer size to limits prescribed by the application.

Fig. 2 displays a generic pulse transformer from top-down and front views, indicating (most importantly) pulse transformer core leg width (x_c), core depth (y_c), winding length (l_w), and isolation distance (d_i). Note that since the two secondary windings are connected in series, the peak voltage of the rightmost winding is only half of the application voltage, i.e. half of the isolation distance required at full voltage may be used, reducing total leakage inductance by roughly 25%. Note also that in high power long pulse applications, damping is naturally high due to low equivalent load impedance and, relatively speaking, long rise times (connected to transformer leakage inductance), equation (1). This significantly simplifies optimization as there is little need to manipulate transformer stray capacitance, i.e. indicated dimensions r and e reduce to d_i.

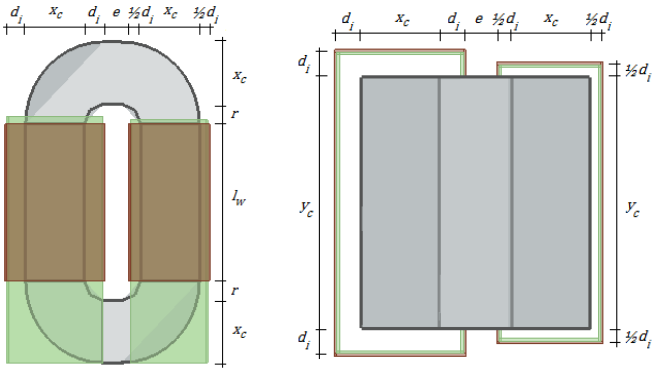

Fig. 2. Generic high voltage pulse transformer, left) front view; right) top-down

$$\zeta = \frac{1}{2R}\sqrt{\frac{L_\sigma}{C_d}} \tag{1}$$

A. Single layer winding technique

The developed optimization procedure for the single layer winding technique is outlined in Fig. 3. Here, the winding is made up of a single layer of standard enameled round copper wire. The simplifications previously outlined reduces the optimization problem to the selection of core leg width, x_c, number of turns per winding, N_2, and distance between winding turns, d_w.

From these design parameters, the entire pulse transformer geometry may be derived as follows. First, transformer core depth is immediately given from the required voltage time integral, equation (2). Further, optimal conductor area may be calculated from application current and maximum current density. For the single layer winding, this allows calculation of wire diameter and hence transformer winding length, equations (3)-(4).

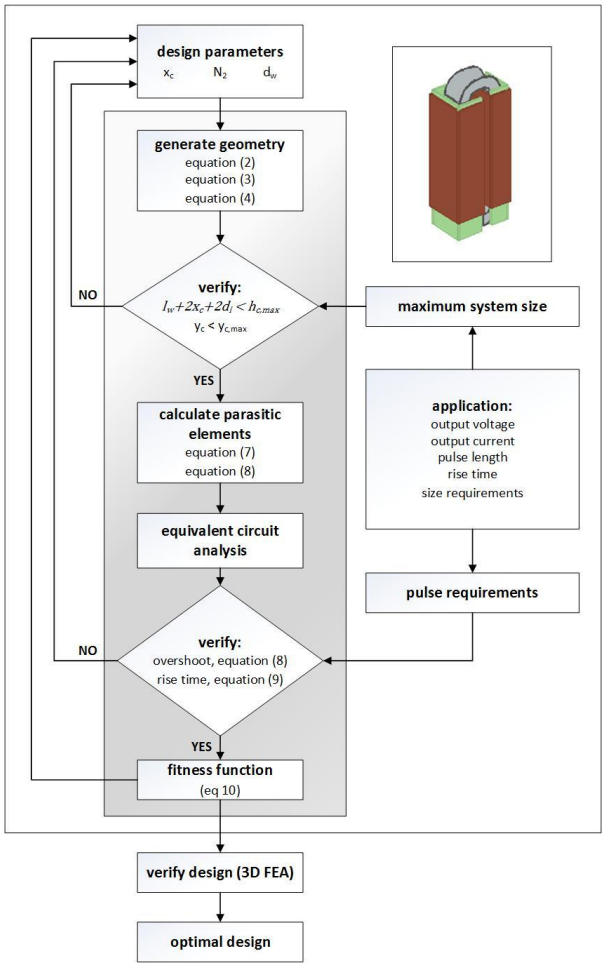

Fig. 3. Outline of developed optimization procedure for pulse transformer based on single layer winding technique

$$V_2 = N\frac{d\emptyset}{dt} = \frac{4N_2\hat{B}x_c y_c k_f}{T_p} \rightarrow y_c = \frac{V_2 T_p}{4N_2\hat{B}x_c k_f} \tag{2}$$

where V_2 is the pulse voltage, T_p is the pulse length, B is the peak magnetic flux density, and k_f is the magnetic fill factor.

$$\emptyset_w = \sqrt{\frac{4I_2\sqrt{T_p f_r}}{J\pi}} \tag{3}$$

$$l_w = N_2\emptyset_w + (N_2 - 1)d_w \tag{4}$$

where Φ_w is the wire diameter, f_r is pulse repetition rate, J is current density, and d_w is the distance between winding turns.

Before calculating resulting pulse characteristics, the generated pulse transformer geometry is checked against imposed size constraints, equations (5)-(6).

$$l_w + 2x_c + 2d_i \le \hat{h}_c \tag{5}$$

$$y_c \le \hat{y}_c \tag{6}$$

If these constraints are satisfied, the procedure continues with calculation of parasitic elements from the transformer geometry. Leakage inductance, linked to the magnetic field energy present between primary and secondary windings [3], is estimated by equation (7).

$$L_\sigma = \mu_0 N_2^2 \frac{A_{2,A} - x_c y_c}{l_w} + \mu_0 N_2^2 \frac{A_{2,B} - x_c y_c}{l_w} \tag{7}$$

where μ_0 is permeability of free space, A_{2A} and A_{2B} are the areas of the leftmost and rightmost secondary windings in Fig. 2b, respectively.

Stray capacitance is linked to the generated electric field present between primary and secondary windings, between the two secondary windings, and between each secondary winding and the oil tank interior. Fig. 4 presents a model of the pulse transformer indicating contributing stray elements, each of which may be calculated through finite element analysis or use of approximative analytic equations. As previously stated, the derived models are intended for use in a looped global optimization procedure, for which reason parallel plate approximation (accounting for varying voltage throughout the windings) is preferred due to computational efficiency, equation (8).

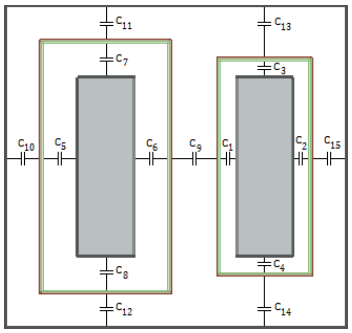

$$C_d = \sum_{i=1}^{15} k_v \varepsilon_0 \varepsilon_r \frac{A_i}{d_i} \tag{8}$$

Fig. 4. Model for calculation of stray capacitance (exaggerated for clarity)

The derived parasitic elements (equations (7)-(8)) are used in forming an equivalent RLC circuit used to determine resulting pulse rise time and pulse overshoot. These are then compared to application requirements, equations (9)-(10).

$$t_r \leq k_r T_p \tag{9}$$

$$\max(v(t)) < k_p V_2 \tag{10}$$

where k_r represents a percentage of the pulse length, and k_p together with V_2 yields the maximum pulse overshoot.

In this study, total weight of magnetic core and copper windings, representing the size of the pulse transformer and, to a certain extent the volume of the oil tank, is optimized, constituting the final step in the optimization procedure. Later, the magnetic core will be seen to generally outweigh the transformer windings significantly, reducing the volume equation to equation (11).

$$V_c = x_c y_c l_c = x_c y_c \left(2l_w + 2d_i + 4\frac{\pi}{2}(x_c/2 + r)\right) \tag{11}$$

Finally, the chosen pulse transformer design is verified in a 3D finite element analysis environment, validating the estimation of the parasitic elements as well as the calculated voltage time integral, pulse overshoot and pulse rise time.

B. Pancake winding technique

In the pancake winding technique a copper strip is wound several layers around the bobbin, one on top of the other, forming a stack. Several stacks are connected in series, constituting a transformer winding. The above outlined optimization procedure may again be used followin modification of equations (3)-(4).

The number of stacks may be pre-determined, i.e. design parameters in addition to core leg width, x_c, are the number of turns as well as stack width, g_w, and stack height, g_h, allowing finer manipulation of leakage inductance. Distance between individual stacks (d_y) is pre-set to allow straightforward series connection between stacks. Consequently, equations (3)-(4) is in this case replaced by equation (12).

$$l_w = g_s g_h + (g_s - 1)d_y \tag{12}$$

Finally, required isolation distance between stack turns, impacting stack width, is given by equation (13).

$$d_x = \frac{V_2}{2N_2} k_i \tag{13}$$

where k_i represents the dielectric strength of the insulating material.

III. Results

In the sections that follow, the developed models and proposed optimization procedure are used to study trends seen in design of pulse transformers for long pulse high power applications as pulse power and pulse length are increased.

A. Evaluation of Trends

Fig. 5 shows the outcome of the procedure for a pulse transformer based on the single layer winding technique. Here, modulator output voltage was set to 115 kV, output current to 25 A, and PRR to 14 Hz. Peak magnetic flux density was set to 1.2 T, magnetic material fill factor to 90%, allowable current density to 5 A/mm^2, and relative permittivity of oil to 2. The pulse length was increased from 500 µs up to 4 ms, from which the allowable 0-99% rise time was given (here 10%). Finally, the height of the pulse transformer was limited to 1.5 m, and the core depth to 1 m.

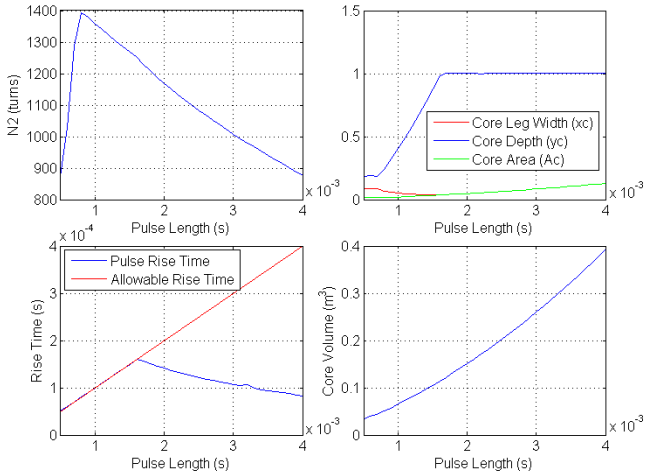

Fig. 5. Trends for pulse transformer based on single layer winding technique

Clearly, in satisfying the voltage time integral condition, equation (2), increasing the number of turns (and as a consequence transformer height) is best in terms of volume, equation (11), followed by increasing core depth and, finally, core leg width. This is demonstrated in this first case, Fig. 5, in which allowable rise time is quite high (10% of pulse length), allowing transformer number of turns to grow linearly in coping with the increasing pulse length (T_p from 500 µs to

800 µs). Consequently, magnetic core area is seen to be essentially constant throughout a first interval.

Eventually, this increase in number of turns is halted by transformer height limitations (T_p = 800 µs), forcing increase in magnetic core area. As a matter of fact, this limitation requires a decrease in number of turns due to increasing RMS current, equation (3). Finally, as core depth reaches its constraint of 1 m (T_p = 1.6 ms), the necessary increase in core leg width forces a decrease of winding length, and therefore an even faster decrease in number of turns, equation (5). As can be seen, this yields a suboptimal pulse rise time (i.e. unnecessarily faster than required by the application at the cost of magnetic core volume) and a quadratic tendency in magnetic core volume. This tendency quickly makes high power long pulse transformers based on the single layer winding technique cumbersome and difficult to maintain, and in some cases unfeasible. It is here remarked that the effects of these tendencies are strongly amplified as shorter rise times and applications of higher power and longer pulse lengths are contemplated, as studied later in this section.

Fig. 6 shows the outcome of the procedure for a pulse transformer based on the pancake winding technique applying the same load parameters and material constants outlined in the beginning of this section. The number of stacks is pre-set to 20, with a distance of 10 mm in between each stack.

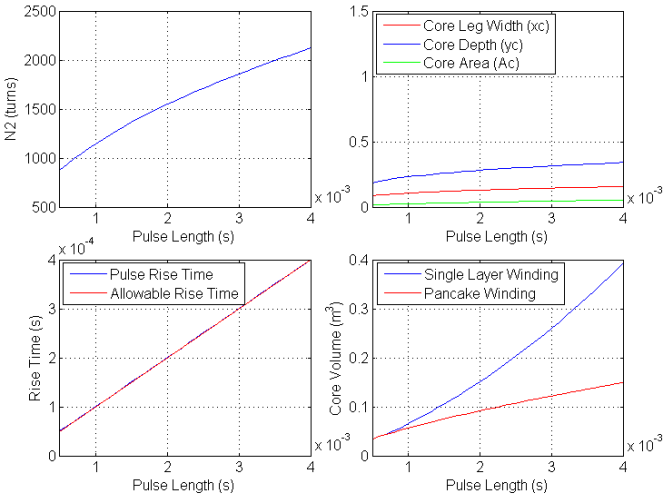

Fig. 6. Trends for pulse transformer based on pancake winding technique

In this case, the limitation on transformer height is not an imposition on increasing number of turns as they are added widthwise. As such, attained rise time always coincides with allowable rise time and magnetic core area increases only very slowly. It is noted that the number of turns does not increase linearly, but is connected to the square root of the pulse length as increasing the number of turns without a corresponding increase in winding length affects the leakage inductance by a square factor, equation (7).

In comparing the core volumes attained using the two winding techniques it is made apparent that equivalent results are obtained for lower pulse lengths. However, when pulse transformer height becomes limited, the pancake winding technique quickly becomes superior as pulse length is further increased. As an example, consider a pulse transformer based on the single layer winding technique intended for a 3.5 ms application, requiring a 0.32 m^3 magnetic core, Fig. 5. The same pulse transformer may be realized using only a 0.13 m^3 magnetic core using the pancake winding technique, Fig. 6, corresponding to an almost 2.5 time reduction in magnetic material.

At which pulse length the above described trends appear and become significant (and whether the intervals overlap or not) is clearly a strong function of allowable pulse transformer height and depth as well as, among other application parameters, modulator load current and allowable rise time.

Fig. 7 plots optimal magnetic core volume for the same application parameters and constraints outlined above. A range of pulse transformer height limitations for both winding techniques are considered. For the single layer winding technique this limit constrains the number of turns and hence when the quadratic tendency in magnetic core volume sets in. Note the strong increase seen in magnetic core volume as height is constrained to 1 m; in this case it becomes physically impossible to produce a pulse transformer for pulse lengths exceeding 3 ms. This trend represents a significant limitation in design as desired pulse length and application power are further increased. Transformers based on the pancake winding technique are, expectedly, almost unaffected by height limitations as additional winding turns are added widthwise.

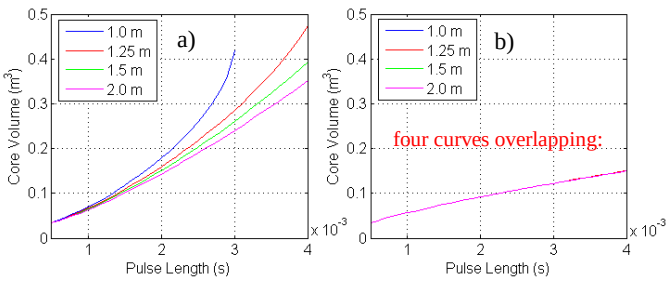

Fig. 7. Optimal magnetic core volume for pulse transformer with varying limitation on pulse transformer height, a) single layer winding; b) pancake winding

Similarly, Fig. 8 plots optimal magnetic core volume for a range of modulator load currents for both winding techniques. Load current determines necessary conductor cross section (and hence number of turns per unit winding length) and is therefore directly connected to the above trends.

As can be seen, for the single layer winding technique magnetic core volume is, comparatively, well represented by a linear function even for longer pulse lengths assuming low load current (e.g. 25 A), whereas the quadratic tendency becomes more pronounced with increasing power. In this case, it becomes impossible to generate a design for supplying 150 A at pulse lengths exceeding that of 3 ms. It should, however, be noted that before pulse length becomes limiting (i.e. in this case 3 ms), magnetic core volume may already be prohibitive – here almost 0.9 m^3 – even with an allowable rise time corresponding to 10% of the pulse length.

Increasing load current also affects the magnetic core volume of transformers based on the pancake winding technique due to a corresponding decrease in allowable leakage inductance (and hence number of turns), forcing an increase in core size. This increase, however, is much more

measured than that seen for the single layer winding technique.

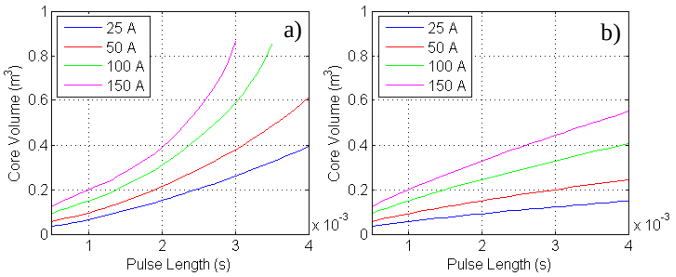

Fig. 8. Optimal magnetic core volume for pulse transformer with varying modulator load current, a) single layer winding; b) pancake winding

Finally, in applications of high average power very short rise times are necessary to ensure high efficiency operation. Clearly, restricted rise time in combination with high power and a reasonable height constraint therefore severely limits the number of turns, implying steep magnetic core volume increase as longer pulse lengths are desired. Fig. 9 shows the outcome of the procedure as applied to a 115 kV, 100 A output pulse as transformer height and depth are constrained to 1.5 m and 1 m, respectively, as allowable rise time is reduced from 10% to 2.86%, representing the requirements of the ESS modulators.

Expectedly, for high power applications with shorter rise times the quadratic tendency seen for the single layer winding technique is delayed. Consequently, the results for both winding techniques are virtually identical, producing equivalent designs throughout the pulse length range assuming a 0-99% rise time no longer than 2.86% of the pulse length. This suggests use of the simpler single layer winding technique, although both options require a magnetic core of 0.9 m^3 at 3.5 ms, corresponding to more than 7000 kg. It should be noted, however, that the pancake winding allows somewhat longer pulse lengths than that of the single layer winding (4 ms as opposed to 3.5 ms). The size constraints could be opened, although at cost of manufacturability and maintainability. These results highlight the difficulties of pulse transformer based approaches for long pulse high power applications with high pulse quality requirements, and will be studied in further detail in a subsequent publication.

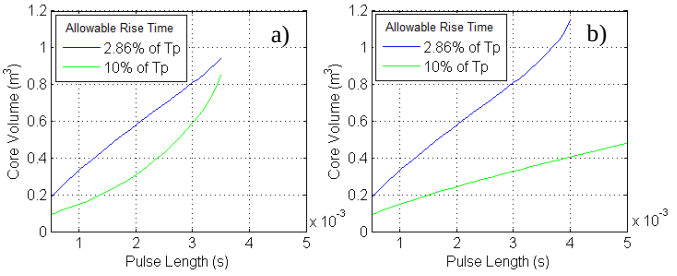

Fig. 9. Optimal magnetic core volume for pulse transformer with varying pulse rise time requirement, a) single layer winding; b) pancake winding

B. Application

In this section, implications of the above studied trends will be demonstrated for a proposed application. Here, a pulse length of 2.8 ms with a maximum 0-99% rise time of 300 µs is needed. Pulse output voltage is expected to be 115 kV, with output current 25 A and PRR 14 Hz. Peak magnetic flux density is allowed to be 1.55 T. Transformer height is in this application limited to only 0.9 m.

Fig. 10 presents the above analysis as applied to this design problem. Due to the strict limitation on transformer height, magnetic core volume for the single layer winding technique increases steeply despite relatively low output current, becoming unfeasible right after application pulse length. Consequently, a pancake winding based pulse transformer is preferred. Table 1 summarizes the final design. Note that a 10% margin in rise time was introduced to meet the required maximum rise time in case of higher obtained leakage inductance (tolerance).

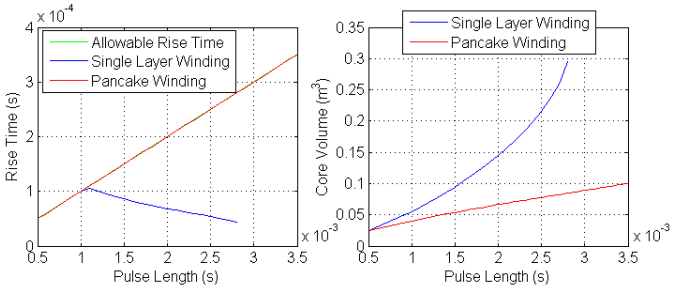

Fig. 10. Design example of 115 kV / 25 A / 14 Hz / 2.8 ms pulse transformer

TABLE I. SUMMARY OF PULSE TRANSFORMER DESIGN

Quantity	Description	Value	Unit
V_p	Output voltage	115	kV
I_L	Load current	25	A
T_p	Pulse length	2.8	ms
PRR	Pulse repetition rate	14	Hz
J	RMS current density	2	A/mm^2
B_{sat}	Peak magnetic flux density	1.55	T
x_c	Core leg width	0.10	m
y_c	Core depth	0.50	m
g_s	No. stacks per leg	22	
g_l	No. layers per stack	45	
C_d	Equivalent stray capacitance	0.353	nF
L_σ	Total leakage inductance	0.281	H
t_r	Rise time	275	µs

The above design was validated in a 3D FEA study, as follows. The geometry summarized in Table 1 was imported to COMSOL® Multiphysics, and simulated first in electrostatic condition to derive a value for the equivalent stray capacitance (C_d) and to validate chosen isolation distances. The system was then analyzed in a time dependent study to validate peak magnetic flux density over time, equation (2), and to simulate the entire output pulse.

In simulating the electric field, the pulse transformer geometry was placed inside an oil tank. The potential was evenly distributed across the two windings, Fig. 11a. Clearly, the majority of the stored energy is found within and around the leftmost (i.e. high voltage) secondary winding. Integrating system energy density over the oil tank volume yields a value for the equivalent stray capacitance C_d = 0.367 nF, within 5% of the value obtained from the developed analytical equation.

The simulated magnetic flux density at the end of the pulse (2.8 ms) is shown in Fig. 11b, and is in the straight sections observed to be 3.11 T. Hence, assuming a properly implemented dc bias power supply, the resulting peak flux

density is at the 1.55 T threshold, indicating proper utilization of the magnetic core. Integrating stored magnetic energy over the oil tank volume (excluding that of the magnetic core) allows calculation of the leakage inductance L_σ = 0.293 H, again seen to be within 5% of the value obtained from developed leakage inductance equation.

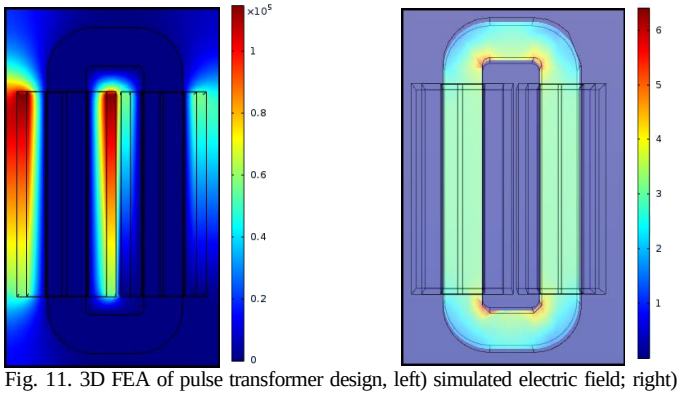

Fig. 11. 3D FEA of pulse transformer design, left) simulated electric field; right) simulated magnetic field at end of pulse (2.8 ms)

Finally, Fig. 12 shows the resulting output pulse voltage for the chosen pulse transformer design. The 0-99% rise time of the pulse is verified to be close to the application specification. The absence of pulse overshoot as well as good agreement (within 5%) among the finite element based calculation and the calculations based on analytical equations demonstrate the low impact of parasitic capacitive elements in long pulse high power applications, and further validate the developed equations for estimating pulse transformer leakage inductance and stray capacitance used in design. It is noted that these results were obtained assuming an ideal primary side switch and a well function droop compensation system (bouncer). Note also that the rise time derived from FEA as expected is slightly higher than those derived analytically (supporting the decision to implement rise time margin).

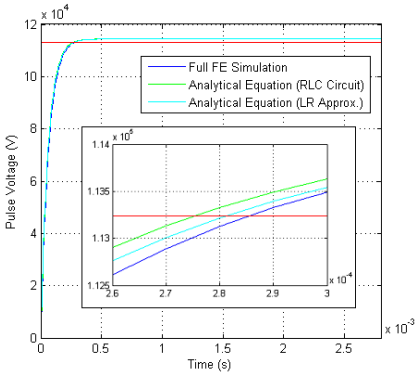

Fig. 12. Output voltage for chosen pulse transformer design

IV. Conclusions

Optimal design models for pulse transformers intended for long pulse high power applications have been presented and used in a procedure to study trends in design parameters and transformer volume (fitness function) as pulse length, pulse power, size constraints, and allowable rise time are varied.

The study in accordance with developed model equations indicates, in minimizing pulse transformer volume, a clear preference to increase transformer number of turns in satisfying the voltage time integral condition, followed by increasing core depth and core leg width. Consequently, if a longer pulse rise time is permitted (10% of pulse length), a pulse transformer based on the single layer winding technique is quickly constrained by the application height limitation, giving rise to suboptimal rise time and a quickly developing quadratic tendency in pulse transformer volume. In this case, the pancake winding technique (although more complex), allowing turns to be added widthwise, typically yields much better results.

In high power applications with requirements on very short rise time the maximum number of turns is strictly limited, mitigating the advantages of the pancake winding technique, yielding identical results. It was demonstrated that an application requiring a 115 kV, 100 A, 14 Hz pulse with 3.5 ms pulse length and a 0-99% rise time not exceeding 100 µs demands a 0.9 m^3 magnetic core. The details of these trends will be studied further in a subsequent publication.

Finally, the procedure was used in considering design choices for a pulse transformer rated for pulse amplitude 115 kV, output current 25 A, pulse length 2.8 ms, and 0-99% rise time <300 µs. The chosen design was validated in a 3D finite element analysis environment.

References

[1] J. Biela; "State-of-the-Art Solid State Pulse Modulators", presented at CERN Accelerator School, Baden, Switzerland, 7-14 May, 2014.

[2] P. Viarouge et al; "Modeling and Dimensioning of High Voltage Pulse Transformers for Klystron Modulators", 2012 Intl. Conf. on Electrical Machine (ICEM), 2-5 Sept. 2012, pp. 2332-2338;

[3] M. Collins et al; "A Modular and Compact Long Pulse Modulator based on the SML Topology", IEEE Trans. On Diel. and Elect. Insul., Vol 24, No 4; Sept. 2017, pp. 2259-2267;

[4] D. Gerber; "Ultra-precise Short Pulse Modulator for a 50 MW RF Output Klystron for Free-electron Lasers", Doctoral Dissertation, ETH Zurich, 2015;

[5] D. Aguglia et al; "Klystron Modulator Technology Challenges for the Compact Linear Collider (CLIC)", 2011 IEEE Pulsed Power Conf. (PPC), 19-23 June, 2011;

[6] S. Blume et al; "Design and Optimization Procedure for High-Voltage Pulse Power Transformers", IEEE Trans. On Plasma Science, Vol 43, No 10; August 2015, pp. 3385-3391;

[7] S. Candolfi; "Finite Element Based Optimal Design Approach for High Voltage Pulse Transformers", IEEE Trans. On Plasma Science, Vol 43, No 6; June 2015, pp. 2075-2080;

[8] S. Blume et al; "Optimal Transformer Design for Ultraprecise Solid State Modulators", IEEE. Trans on Plasma Science, Vol 41, No 10; October 2013, pp. 2691-2700;

[9] D. Habibinia et al; "Optimal Winding Design of a Pulse Transformer considering Parasitic Capacitance Effect to reach best Rise Time and Overshoot", IEEE Trans. on Diel. and Elect. Insul., Vol 21, No 3; June 2014, pp. 1350-1359;

[10] Y. Wang et al; "Optimal Design and Experimental Study of Pulse Transformers with Fast Rise Time and Large Pulse Duration", IEEE Trans. On Plasma Science, Vol 42, No 2; February 2014, pp. 300-306;

[11] S. Peggs et al; "European Spallation Source Technical Design Report". Internet: https://europeanspallationsource.se/sites/default/files/downloads/2017/09/TDR_online_ver_all.pdf, April 23, 2013 [March 11, 2018];

[12] R. Kustom; "An Overview of the Spallation Neutron Source Project", 20th Intl. Linear Accelerator Conference (LINAC2000), 21-25 Aug. 2000